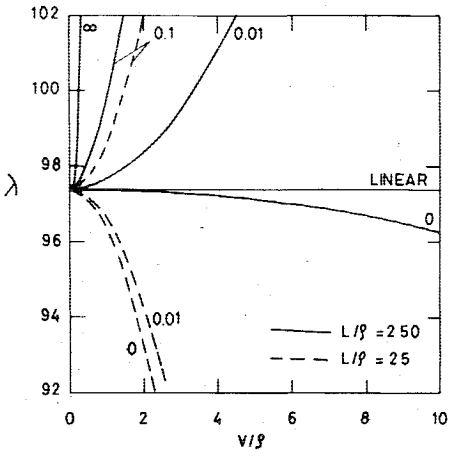

Fig. 2 λ-amplitude relationship.

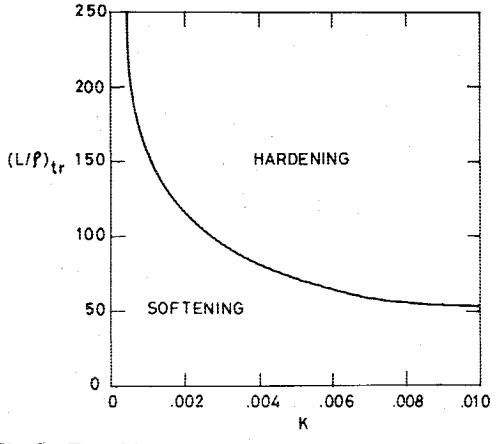

Fig. 3 Transition slenderness ratios vs spring constant.

sition value of (L/ρ) is plotted in Fig. 3 as a function of K. Thus we identify clearly a regime of a hardening type of nonlinear behavior and another of a softening type, depending on (L/ρ) and (kL/EA_0), for a uniform beam.

V. Conclusions

Whereas all previous analyses have studied the problem in the hardening regime alone[1-5,9] or in the softening regime alone,[6-8] this Note unifies both formulations. The variable axial restraint at the boundary is seen to play an important role in determining the nonlinear dynamic behavior of the beam. From the present results and earlier conclusions,[1-9] one may conclude that the principal causes and effects of nonlinearity are a hardening effect due to axial stretching, use of exact curvature expressions, and equilibrium equations, and a softening effect due to longitudinal inertia forces. At low values of spring constant and slenderness ratios, the effect of longitudinal inertia predominates, whereas, at high values of axial restraint and slenderness ratios, the effect of axial stretching predominates.

Acknowledgment

The author is deeply indebted to K. A. V. Pandalai and T. K. Varadan for their constant encouragement and interest in the subject.

References

[1] Woinowsky-Krieger, S., "The Effect of an Axial Force on the Vibration of Hinged Bars," *Journal of Applied Mechanics*, Vol. 17, 1950, pp. 35-36.

[2] Eringen, A., "On the Nonlinear Vibrations of Thin Bars," *Quarterly of Applied Mathematics*, Vol. 9, 1952, pp. 361-369.

[3] Burgreen, D., "Free Vibration of a Pin-Ended Column with Constant Distance Between Ends," *Journal of Applied Mechanics*, Vol. 18, 1951, pp. 135-139.

[4] Srinivasan, A. V., "Large Amplitude Free Oscillations of Beams and Plates," *AIAA Journal*, Vol. 3, Oct. 1965, pp. 1951-1953.

[5] Raju, I. S., Venkateshwara Rao, G., and Kanaka Raju, K., "Large Amplitude Free Vibrations of Tapered Beams," *AIAA Journal*, Vol. 14, Feb. 1976, pp. 280-282.

[6] Bolotin, V. V., *Dynamic Stability of Elastic Systems*, Holden-Day, 1964.

[7] Genin, J. and Radwan, H., "Nonlinear Bending Inertia of a Vibrating Beam," *Zeitschrift für Angewandte Mathematik und Physik*, Vol. 21, 1970, pp. 983-990.

[8] Atluri, S., "Nonlinear Vibrations of a Hinged Beam Inlcuding Nonlinear Inertia Effects," *Journal of Applied Mechanics*, Vol. 40, 1973, pp. 121-126.

[9] Wrenn, B. G. and Mayers, J., "Nonlinear Beam Vibrations with Variable Axial Boundary Restraint," *AIAA Journal*, Vol. 8, Sept. 1970, pp. 1718-1720.

[10] Prathap, G., "Nonlinear Behavior of Flexible Bars, Anisotropic Skew Plates and Stiffened Plates," Ph.D. Dissertation, Indian Inst. of Technology, Madras, India, 1977.

[11] Prathap, G. and Varadan, T. K., "Nonlinear Vibrations of Tapered Cantilevers," *Journal of Sound and Vibration*, Vol. 55, Jan. 1977.

[12] Prathap, G. and Varadan, T. K., "Large Amplitude Free Vibration of Tapered Hinged Beams," *AIAA Journal*, Vol. 16, Jan. 1978, pp. 88-90.

Radiometer Force on the Proof-Mass of a Drag-Free Satellite

Robert E. Jenkins*
The Johns Hopkins University, Laurel, Md.

Introduction

In recent years there has been increasing activity and interest in the use of "drag-free" and "accelerometric" satellites. Both of these devices make use of a proof-mass floating within a cavity, which is shielded by the cavity from air drag and solar radiation pressure forces. The idea was first proposed by Lange,[1] who also proposed various applications for such satellites.

The drag-free satellite is equipped with thrusters on the main satellite body which are operated by closed-loop control to keep the satellite body centered on the proof-mass. The entire spacecraft then, in principle, flies a purely gravitational orbit. The first such spacecraft, TRIAD (1972-69A), was successfully orbited by Johns Hopkins University/Applied Physics Lab in 1972.[2,3] The drag compensation system on TRIAD was based on a spherical, gold proof-mass in a spherical cavity, using a capacitance measurement to sense its position. A different, single-axis system has been recently orbited which is based on a doughnut-shaped proof-mass sliding along a wire. The proof-mass is suspended off the wire by radial magnetic forces, and its position is sensed optically. This system was used on the TIP Navigation Satellite launched in 1977.

In the accelerometric satellite, there is no thrusting system on the main body. Instead, a closed-loop control system maintains the proof-mass at the center of the cavity by means of an electrostatic internal force between the proof-mass and cavity. Ideally, this force just balances the external surface

Received Dec. 12, 1977; revision received Feb. 24, 1978. Copyright © American Institute of Aeronautics and Astronautics, Inc., 1978. All rights reserved.

Index categories: Spacecraft Dynamics and Control; Spacecraft Navigation, Guidance, and Flight-Path Control.

*Principle Professional Staff, Applied Physics Laboratory.

forces, and a knowledge of its magnitude constitutes a precise measurement of the surface forces. The first spacecraft of this type was the CASTOR Satellite (1975-39B), launched by the French space agency CNES. This system, called CACTUS, used a spherical proof-mass of platinum and capacitive position sensing.[4,5]

In practice, with either type of device, operating imperfections are introduced by any internal force perturbation on the proof-mass. These internal force biases are one of the most important, if not the dominant design consideration, in building the devices. The problem of controlling internal forces is difficult simply because they must be reduced to quite small levels to achieve useful operating capability. The design goal on TRIAD, for example, was to limit the internal biases to 10^{-11} g. On the CASTOR spacecraft the design goal was better than 10^{-9} g.

There are various sources for internal biases which were carefully considered during the design of both types of systems. These include: 1) gravitational attraction of the proof-mass by the main satellite body; 2) magnetic forces caused by an induced or residual dipole in the proof-mass interacting with nearby current loops; and 3) electrostatic forces arising from a charge build-up on the proof-mass relative to the main body.

In some cases, the stability of the internal forces is the important consideration, rather than the magnitude of the force. For example, in a drag-free satellite that is 3-axis stabilized, the presence of a constant internal force causes an orbital effect which can be modeled. Then, the bias force can be estimated as part of the orbit determination process and thus be properly accounted for in generating the satellite ephemeris. Only the variability of the bias would cause a serious problem in this case.

The electrostatic problem is particularly difficult and has received some attention in recent literature. Reference 6 is an interesting study of proof-mass charge built-up, and it presents evidence for this phenomenon using the orbital performance data of the CACTUS system. In retrospect, it appears that the orbital performance of the TRIAD system[3] showed evidence of charge build-up.

Radiometer Force

Another potential source of internal force bias—the radiometer force arising from a low-pressure gas within the cavity is now discussed. The radiometer effect results from a temperature gradient in a very low-pressure gas. The gas in the cavity could result from outgassing of the materials within the cavity and from the cavity walls themselves. If the cavity is closed or has only small openings, the gas will escape by diffusion. The diffusion rates in balance with the outgasing rates could result in an equilibrium pressure within the cavity that is significantly higher than the pressure outside the spacecraft, and this could persist for a matter of months or more. The same thing could result if the spacecraft outer shell were completely closed.

With a temperature difference at the walls on opposite sides of the cavity, the gas will pick up that temperature gradient in collisions with the walls if there is any accommodation of the gas molecules on the walls. Also, the outgassed molecules can be emitted at different temperatures if there is sufficient temperature difference across the package. The resulting temperature gradient in the gas around the proof-mass gives rise to the radiometer force on the proof-mass.

The problem can be further complicated by an appreciable temperature gradient across the proof-mass itself if there is any accommodation of the gas on the ball. This effect has been neglected because it is felt that the gas collisions with the proof-mass would be mainly elastic considering its likely material composition.

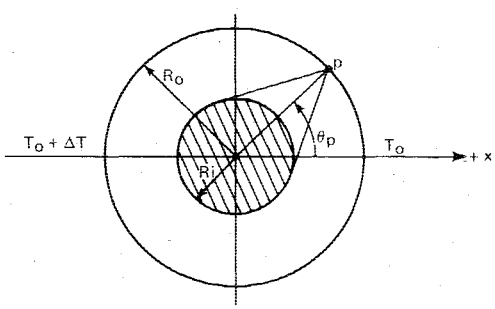

Fig. 1 Spherical proof-mass and cavity with temperature gradient.

Estimate of Magnitude of the Force

Reference 7 gives a rigorous treatment of the radiometer effect using the so-called "dusty gas model," which was first used to analyze gases containing large suspended particles. In this model, the solid (i.e., proof-mass) is treated as one component of a gas mixture, and then the rigorous Chapman-Enskog gaseous diffusion equations are used to describe the system.

From this treatment, Ref. 7 gives the following formula for the radiometer force on a solid body in the low-pressure gas:

$$\frac{F}{V} = \frac{\pi_1 \pi_2 P}{2(\pi_1 + P)(\pi_2 + P)} \nabla \ell_n T \tag{1}$$

where F/V is the force per unit volume in the direction of the temperature gradient $\nabla \ell_n T$, P is the pressure, and π_1 and π_2 are physical constants with units of pressure. They are given by

$$\pi_1 = 3kT\eta/2mD \qquad \pi_2 = \eta D R_0 \tag{2}$$

where η is the gas viscosity, k is the Boltzman constant, D is the Knudsen diffusion coefficient for the gas on the solid body, m is the gas molecule mass, and R_0 is a geometrical constant arising from Stokes law.

Both D and R_0 are geometry dependent and D depends on the details of the molecular scattering off the solid. For a spherical proof-mass and elastic hard-sphere scattering, it can be shown that[7]:

$$\pi_1 \approx \pi_2 = 0.1(kT/r) \tag{3}$$

where r is the proof-mass radius. In this case, Eq. (1) shows a maximum at a value of $P \approx \pi_1 \approx 2 \times 10^{-3}$ mm hg,

$$a = \frac{F}{V\rho} = \frac{0.1k\Delta T}{8r^2\rho} \tag{4}$$

where ρ = the proof-mass density (about 20 g/cm^3 for gold). For $P \ll \pi_1$, in the free molecular region, Eq. (1) reduces to the limiting form

$$a = \frac{P}{2\rho} \nabla \ell_n T = \frac{P\Delta T}{4\rho r T} \tag{5}$$

assuming $\nabla \ell_n T = \Delta T/2rT$.

Except for the approximations to the geometrical constants, Eq. (1) and hence Eq. (5) should be a rigorous result, but the physics are unfortunately rather obscure. To test the qualitative nature of Eq. (5) and to understand the physics a bit better, we can resort to a simple model based on free molecules.

Assume a spherical proof-mass inside a spherical cavity where there is total accommodation on the cavity walls with the gas molecules emitted at the wall temperature. Referring to Figs. 1 and 2, consider a point p on the outer sphere with angular coordinates θ_p, φ_p emitting molecules toward a point p' on the ball. In equilibrium, the number of molecules that

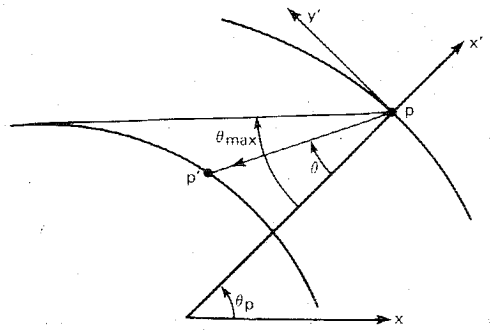

Fig. 2 Geometry for molecules originating at point on cavity.

hit the wall are just balanced by the re-emitted molecules, so a point on the wall acts in a sense just like a point in the gas where the flux through an elemental area is the same in both directions.

The flux of molecules through p with velocity v in the direction $p-p'$ is given by:

$$J=nvf(v,T)v^2\mathrm{d}v\ \sin\theta\ \mathrm{d}\theta\ \mathrm{d}\varphi \tag{6}$$

where n is the number density of molecules in the cavity, and $f(v,T)$ is the Maxwellian distribution function. The limits on θ and φ in Eq. (6) are:

$$0\le\varphi\le 2\pi \text{ and } 0\le\theta\le\theta_{\max} \tag{7}$$

where

$$\theta_{\max}=\sin^{-1}(R_i/R_0)$$

By symmetry, it can be seen that the total force on the ball from the molecules emitted at point P must be in the $-x'$ direction shown in Fig. 2. For an elastic collision at p', it can be shown that the momentum transported to the ball in the x direction is given by

$$\Delta P_x=-2mv(\cos\theta-K^2\sin^2\theta\cos\theta$$
$$+K\sin^2\theta\sqrt{1-K^2\sin^2\theta})\cos\theta_p \tag{8}$$

where $K=R_0/R_i$. Hence, the x component of the force on the ball, originating from the molecules emitted from an elemental area at point p, is given by

$$\mathrm{d}F_x=\int J\Delta P_x \tag{9a}$$

$$\mathrm{d}F_x=\int_0^{\infty}\mathrm{d}v\int_0^{\theta_{\max}}\mathrm{d}\theta\int_0^{2\pi}\mathrm{d}\varphi nv^4f(v,T)\sin\theta\Delta P_x$$
$$\cdot R_0^2\sin\theta_p\mathrm{d}\theta_p\mathrm{d}\varphi_p \tag{9b}$$

where

$$f(v,T)=\left(\frac{m}{2\pi kT}\right)^{3/2}\exp\left(\frac{-mv^2}{2kT}\right) \tag{10}$$

and T is the temperature of the wall at point p.

Performing the first three integrals in Eq. (9b), and then integrating over all points on the cavity wall, we get

$$F_x=-\frac{3}{2}nkR_i^2\int_0^{2\pi}\mathrm{d}\varphi_p\int_0^{\pi}\mathrm{d}\theta_p T\sin\theta_p\cos\theta_p \tag{11}$$

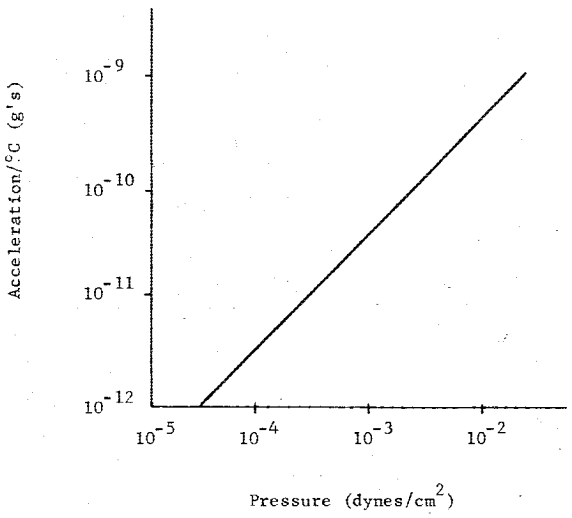

Fig. 3 Acceleration of proof-mass per 1°C temperature gradient (gold proof-mass of 2 cm radius at 300 K).

We now assume that T is given as a simple function of θ_p

$$T=T_0-\frac{\mathrm{d}T}{\mathrm{d}x}R_0\cos\theta_p \tag{12}$$

where $\mathrm{d}T/\mathrm{d}x$ is a (constant) temperature gradient in the x direction. The final integration gives

$$F_x=2\pi nkR_i^2R_0\frac{\mathrm{d}T}{\mathrm{d}x} \tag{13}$$

or

$$a=\frac{F_x}{V\rho}=\frac{3}{2}\frac{nkR_0}{\rho R_i}\frac{\mathrm{d}T}{\mathrm{d}x}=\frac{3}{2\rho}\frac{R_0}{R_i}\frac{P}{T}\frac{\mathrm{d}T}{\mathrm{d}x} \tag{14}$$

which is in qualitative agreement with Eq. (5).

For a gold proof-mass with a 2-cm radius, the numerical value given by Eq. (5) is shown in Fig. 3 as a function of gas pressure at 300 K for a 1°C temperature gradient across the proof-mass. The effect clearly is not important unless the pressure in the cavity is at least 10^{-5} dyn/cm^2. This is about the ambient pressure at 400 km altitude during low solar activity. If the cavity were closed tightly enough to sustain an internal pressure significantly higher than ambient, the radiometer effect could be serious. At altitudes below 400 km, the ambient pressure alone could be enough to cause a significant bias.

References

[1] Lange, B. O., "The Drag Free Satellite," *AIAA Journal*, Vol. 2, Sept. 1964, pp. 1590-1606.

[2] *APL Technical Digest*, Vol. 12, June 1973, entire issue.

[3] Space Department, Applied Physics Lab. and the Guidance and Control Laboratory, Stanford University, "A Satellite Freed of all but Gravitational Forces: TRIAD," *Journal of Spacecraft and Rockets*, Vol. 11, Sept. 1974, pp. 637-644.

[4] "Les Essais en Orbite de L'Accéléromètre Cactus," Paper 1976-5, Office National D'Etudes de Recherches Aerospatiales, Chatillon, France.

[5] Bourtes, J., et al., "Qualifications in Orbital Flight of the Cactus High Sensitivity Accelerometer," presented at the 19th COSPAR Meeting, Philadelphia, June 1976.

[6] Juillerat, R. and Philippon, J., "Electrification of the Proof-Mass of a Drag Free or Accelerometric Satellite," presented at the Conference on Technology of Electric Charge in Space, Colorado Springs, Oct. 1976; also ONERA Paper no. 1976-150.

[7] Mason, E. A. and Block, B., "Molecular Collision Cross Sections from the Radiometer Force," *Annals of Physics*, Vol. 37, 1966.